Global analysis of asymmetric RNA enrichment in oocytes reveals low conservation between closely related *Xenopus* species

Maike Claußen[a], Thomas Lingner[b], Claudia Pommerenke[b,*], Lennart Opitz[b,†], Gabriela Salinas[b], and Tomas Pieler[a]

[a]Institute of Developmental Biochemistry and [b]Microarray and Deep-Sequencing Core Facility, University Medical Center Göttingen, 37077 Göttingen, Germany

ABSTRACT **RNAs that localize to the vegetal cortex during *Xenopus laevis* oogenesis have been reported to function in germ layer patterning, axis determination, and development of the primordial germ cells. Here we report on the genome-wide, comparative analysis of differentially localizing RNAs in *Xenopus laevis* and *Xenopus tropicalis* oocytes, revealing a surprisingly weak degree of conservation in respect to the identity of animally as well as vegetally enriched transcripts in these closely related species. Heterologous RNA injections and protein binding studies indicate that the different RNA localization patterns in these two species are due to gain/loss of *cis*-acting localization signals rather than to differences in the RNA-localizing machinery.**

Monitoring Editor
Marvin P. Wickens
University of Wisconsin

Received: Feb 26, 2015
Revised: Aug 7, 2015
Accepted: Aug 28, 2015

INTRODUCTION

The closely related Pipid species *Xenopus laevis* (African clawed frog) and *Xenopus (Silurana) tropicalis* (western clawed frog) are members of two different clades of the *Xenopus* genus, originating from a common ancestor ~50 million years ago (Bewick *et al.*, 2012). Whereas *X. laevis* is allotetraploid, with 18 chromosome pairs and a genome size of 3.1 GB, *X. tropicalis* has a diploid karyotype, with 10 chromosome pairs and a genome size of 1.7 GB (Sater, 2012). A high degree of conservation has been described for the coding regions of orthologous genes in *X. laevis* and *X. tropicalis* (90% sequence identity; Yanai *et al.*, 2011). Comparative transcriptome analysis revealed strongly conserved gene expression for the majority of orthologues, with changes affecting mainly the transcript levels rather than differences in the temporal profile of expression. Largest differences in expression levels were observed for maternally supplied transcripts (Yanai *et al.*, 2011).

mRNA localization is understood to play an important role in early embryonic patterning and cell fate determination. In *X. laevis*, vegetally localized maternal mRNAs were found to be crucial for germ cell development and germ layer formation in the early embryo (King *et al.*, 2005). Vegetal RNA localization in *Xenopus* oocytes is achieved by two major pathways. Early-pathway localization is initiated during the earliest stages of oogenesis by the entrapment of a subpopulation of mRNAs in the germplasm containing mitochondrial cloud, also referred to as Balbiani body; such RNAs become restricted to a relatively narrow region at the tip of the vegetal cortex, overlapping with the germplasm, and many such early pathway mRNAs have been found to be critical for proper germ cell development and migration (Houston, 2013). Late-pathway RNAs translocate toward the vegetal cortex at stages III–IV of oogenesis. In contrast to early-pathway RNAs, late-pathway transcripts localize to a much broader region of the vegetal cortex and function mainly during germ layer formation and patterning in the early embryo (White and Heasman, 2008). These two main localization pathways differ in the underlying mechanisms that drive vegetal enrichment. Whereas association of germplasm RNAs with the mitochondrial cloud is achieved by passive diffusion and entrapment, late-pathway RNAs are actively transported to the vegetal cortex and require dynein as well as kinesin motor proteins for proper localization (Betley *et al.*, 2004; Chang *et al.*, 2004; Messitt *et al.*, 2008; Gagnon *et al.*, 2013). In addition to the RNAs that associate with the vegetal

This article was published online ahead of print in MBoC in Press (http://www.molbiolcell.org/cgi/doi/10.1091/mbc.E15-02-0115) on September 2, 2015.

Present addresses: *DSMZ–German Collection of Microorganisms and Cell Cultures, 38124 Braunschweig, Germany; †Functional Genomics Center Zurich, Swiss Federal Institute of Technology, 8057 Zurich, Switzerland.

Address correspondence to: Maike Claußen (mclauss1@gwdg.de), Tomas Pieler (tpieler@gwdg.de).

Abbreviations used: ISH, in situ hybridization; qPCR, quantitative reverse transcription PCR; UTR, untranslated region.

cortex, a separate group of RNAs are enriched in the animal hemisphere of the oocyte, revealing a more diffuse distribution pattern (reviewed in King *et al*., 2005). The molecular mechanisms by which animal enrichment is achieved are largely unknown (Imbrie *et al*., 2012; Snedden *et al*., 2013).

RNA localization during anuran oogenesis has been most extensively studied in the Pipid *X. laevis* but has also been described to occur in *Rana pipiens* and *Eleutherodactylus coqui*, members of the Ranidae and Eleutherodactylidae families, respectively, which separated from the Pipidae ~200 million years ago (Bossuyt and Roelants, 2009). However, vegetal localization of germ layer determinants such as *vegt* got lost in *E. coqui* after separation from the Ranidae ~150 million years ago (Beckham *et al*., 2003; Bossuyt and Roelants, 2009). The mechanism by which germplasm RNAs such as *dazl* and *ddx25* translocate to the vegetal cortex will differ in these species, since *R. pipiens* and *E. coqui* oocytes appear to be devoid of a mitochondrial cloud (Nath *et al*., 2005; Elinson *et al*., 2011).

RNA localization has also been reported to occur in the oocytes of the teleost *Danio rerio*. As in *Xenopus*, individual germplasm RNAs are transported via the Balbiani body to the oocyte vegetal cortex (Maegawa *et al*., 1999; Howley and Ho, 2000), and zebrafish RNAs localizing to the animal pole during late stages of oogenesis have also been described (Bally-Cuif *et al*., 1998; Houston, 2013). However, RNA localization does not seem to be strongly conserved between zebrafish and *Xenopus*, since several RNAs have been identified that localize in the zebrafish but not in the frog and vice versa (Bally-Cuif *et al*., 1998; Suzuki *et al*., 2000; Kosaka *et al*., 2007).

In the context of this study, we report on a comparative, genome-wide analysis for differentially localizing RNAs in *X. laevis* and *X. tropicalis* oocytes with RNAs isolated from vegetal or animal oocyte halves, respectively. Although we were able to identify a large group of novel vegetally localizing and animally enriched RNAs, there is only a very low degree of conservation with respect to the identity of individual such RNAs in a comparison between the two closely related *Xenopus* species. Furthermore, heterologous RNA localization assays and protein binding studies indicate that this is due to alterations in the RNA signal sequences rather than to differences in the RNA localization machinery.

RESULTS

Global RNA sequencing analysis identifies a large number of novel vegetally localizing transcripts in *X. laevis* oocytes

To achieve a global analysis of differentially localizing RNAs in *X. laevis* and *X. tropicalis* oocytes, we analyzed RNA preparations from animal and vegetal oocyte halves by next-generation sequencing. Sequences obtained were aligned to the transcript reference sequence collection of *X. tropicalis* and analyzed for differential enrichment in either hemisphere. With the exception of the noncoding *xlsirts* and *gptl1* RNAs, which were not detected in the analysis, as well as *exd2* and *ldlrap1*, all other *X. laevis* transcripts that were previously reported and proven to localize to the vegetal cortex by whole-mount in situ hybridization were also found to be significantly enriched in the vegetal hemisphere (Kloc *et al*., 1993; Zhou *et al*., 2004; Kataoka *et al*., 2005; Cuykendall and Houston, 2010; Supplemental Table S1). The degree of enrichment varies between a $\log_2$ fold change (FC) of 8.3 and 1.3. Selected transcripts (*gdf1/vg1*, *dnd1*, and *vegt*) were also analyzed by quantitative PCR (qPCR) and showed excellent quantitative correlation with the deep sequencing data (Supplemental Table S1). Depending on the stringency of the threshold applied, an additional 114 ($\log_2$FC ≥ 2) or 324 ($\log_2$FC ≥ 1) vegetally enriched RNAs were identified (Supplemental Table S2). We noticed considerable overlap of candidate genes identified in this study with those from two previously performed microarray-based screens for vegetally localizing RNAs in *X. laevis* oocytes (Horvay *et al*., 2006; Cuykendall and Houston, 2010; our unpublished results). An arbitrary selection of 34 novel candidate genes was assayed for vegetal localization by means of whole-mount in situ hybridization (Figure 1, Figure 4 later in this article, and Supplemental Figure S1). Of these, 14 were found to localize via the early and 12 via the late pathway. Although they were significantly enriched ($\log_2$FC between 2.25 and 5.02), the remaining eight clones were not found to localize or gave only weak signals. It could be that these RNAs are significantly enriched in the vegetal hemisphere but not associated with the vegetal cortex or germplasm. In summary, this RNA sequencing analysis confirms vegetal enrichment of previously published transcripts and yields a high number of novel, vegetally localizing RNAs that travel either the early or the late pathway in *Xenopus* oocytes.

RNA sequencing identifies many novel but not the previously known animally enriched RNAs in *X. laevis* oocytes

Surprisingly, fewer than one-third of the previously described animally localizing RNAs were found to be enriched in the animal hemisphere above a threshold of twofold ($\log_2$FC ≤ -1), and none of them had more than fourfold enrichment according to the RNA sequencing data (Supplemental Table S3). Lack of animal enrichment was further confirmed by quantitative reverse transcription PCR (qPCR) analysis for *zfand4* and *ddx3x* (previously known as An1 and An3; Rebagliati *et al*., 1985; Gururajan *et al*., 1991; Linnen *et al*., 1993; Supplemental Table S3). On the other hand, deep sequencing analysis revealed a list of novel candidate RNAs with enrichment in the animal hemisphere: 338 with at least twofold and 51 with at least fourfold enrichment (Supplemental Table S4). Four of the novel animally enriched RNAs from *X. laevis* oocytes were selected for qPCR analysis and revealed very similar $\log_2$FC values as obtained by deep sequencing analysis (Figure 2A). To further verify animal enrichment, we cloned cDNA fragments of randomly selected candidate RNAs and performed in situ hybridization with staged *X. laevis* oocytes. Eight of 12 RNAs analyzed were enriched in the animal hemisphere (Figure 2 and Supplemental Figure S2). The remaining four RNAs tested had only very weak signals in the in situ hybridization, precluding classification as animally enriched. The animally enriched RNAs were either homogenously distributed within the animal cytoplasm or enriched within the perinuclear region rather than being restricted to the cortex. In summary, this study allows for the definition of a substantial group of novel, animally enriched RNAs, but it fails to verify many of the previously identified ones.

The identity of differentially localizing mRNAs is only weakly conserved in a comparison of the two closely related species *X. laevis* and *X. tropicalis*

Similar to what we described for *X. laevis,* we also searched for vegetally localizing and animally enriched RNAs in oocytes from *X. tropicalis*. This analysis resulted in the definition of groups of RNAs with numbers very similar to what was observed for *X. laevis* (Supplemental Tables S5 and S6). In general, only about half of the transcripts that were classified to be vegetally localizing were shared between the two species, regardless of whether a relatively low threshold ($\log_2$FC ≥ 1) or a more stringent one ($\log_2$FC ≥ 2) was applied (Figure 3A and Supplemental Table S7). Similarly, the analysis of animally enriched RNAs in *X. tropicalis* also found an equally small overlap with animally enriched RNAs from *X. laevis* (Figure 3B and Supplemental Table S8). Scatterplot

A

Pathway	JgiID	gene symbol/identifier	log2FC
early	Xetrov72021968	*gplt/DY566077*	7,88
	Xetrov72008415	*srgap3*	4,72
	Xetrov72019270	*mov10*	4,18
	Xetrov72010257	*nat6*	3,67
	Xetrov72003748	*tuft1*	3,57
	Xetrov72003321	BJ625728	3,07
	Xetrov72004606	*armc5*	2,87
	Xetrov72037392	EB732697	2,61
	Xetrov72001906	*ppp1r2*	2,51
	Xetrov72034537	*trib1*	2,51
	Xetrov72033461	*sulf1*	2,47
	Xetrov72028947	*fndc3a*	2,35
	Xetrov72029018	*cnksr2*	2,33
	Xetrov72024607	*znf568*	1,61
late	Xetrov72026885	*pgam1*	3,98
	Xetrov72008490	*fam65a*	3,66
	Xetrov72036599	*sox7*	3,63
	Xetrov72007838	*slc12a9*	3,45
	Xetrov72021943	*fam109a*	3,17
	Xetrov72006627	*farp2*	3,17
	Xetrov72010520	*tob2*	2,93
	Xetrov72041496	CA971768	2,87
	Xetrov72032386	NM_001091230	2,83
	Xetrov72025901	*chek1*	2,39
	Xetrov72024723	*atrx*	2,37
	Xetrov72008261	*magi1*	2,25
not localized/ low expression	Xetrov72017571	*snai1*	5,02
	Xetrov72022029	*arl9*	3,49
	Xetrov72032109	BI478312	2,78
	Xetrov72008682	*pkp3*	2,72
	Xetrov72008652	CB205926	2,58
	Xetrov72016346	AW637570	2,57
	Xetrov72027069	*ddit4*	2,36
	Xetrov72010369	*lurap1*	2,25

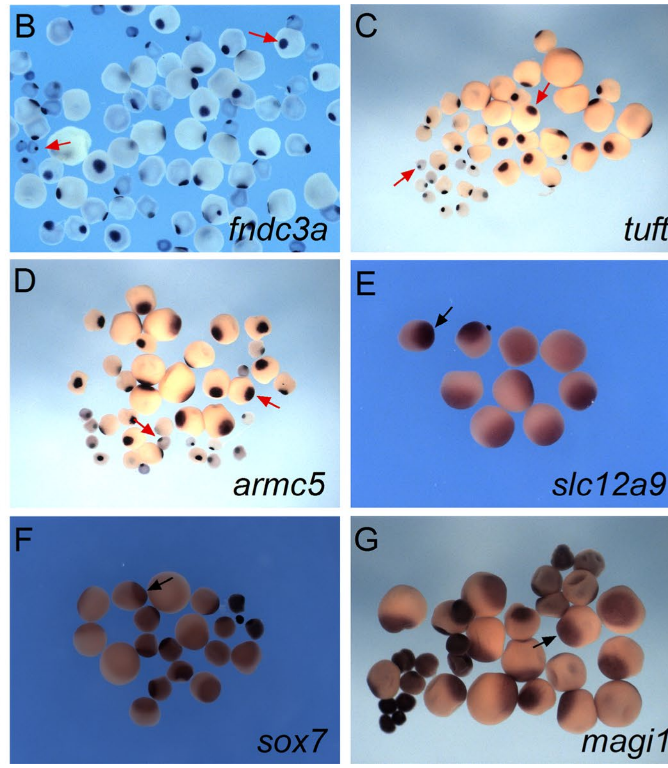

FIGURE 1: Identification of novel vegetally localizing RNAs in *X. laevis* oocytes. (A) Candidate RNAs were tested for vegetal localization by in situ hybridization with *X. laevis* oocytes and listed according to their localization pattern (early and late). JgiID and gene symbol/GenBank accession number, as well as relative enrichment in the vegetal hemisphere as revealed by deep sequencing analysis (expressed as $\log_2$FC). RNAs for which no vegetal localization was detectable by in situ hybridization, as well as RNAs with very low expression levels that did not allow for the determination of localization patterns, are also listed. (B–D) Early-pathway localization pattern with characteristic mitochondrial cloud staining and spatially restricted localization at the vegetal pole (red arrows) for *fnd3ca*, *tuft*, and *armc5* in stage I/II oocytes. (E–G) Late-pathway localization with typical broader vegetal cortex staining (black arrows) for *slc12a9*, *sox7*, and *magi1* in stage III/IV oocytes.

analysis of mean normalized counts per million for vegetal and animal samples indicate comparable general distributions of data points for *X. laevis* and *X. tropicalis*, with an enrichment of genes exhibiting higher expression levels in the group of vegetally enriched transcripts (Supplemental Figure S3).

Conservation of vegetal RNA localization was verified for several transcripts by in situ hybridization, using species-specific probes on *X. laevis* and *X. tropicalis* oocytes, respectively. Transcripts classified to localize to the vegetal cortex in both species were verified for two novel and two previously known genes in both *X. laevis* and *X. tropicalis* oocytes (Figure 4A). Four different RNAs found to be vegetally enriched in *X. laevis* but not in *X. tropicalis* were verified to localize to the vegetal cortex in *X. laevis* oocytes only (Figure 4B). Finally, four RNAs vegetally enriched only in *X. tropicalis* indeed localize in *X. tropicalis* but not *X. laevis* oocytes (Figure 4C). Species-specific vegetal enrichment was also analyzed and confirmed by qPCR for a subset of the foregoing transcripts (Table 1). In summary, we conclude that vegetal localization and animal enrichment of maternal mRNAs are only weakly conserved in a comparison of *X. laevis* and *X. tropicalis*.

Furthermore, gene ontology (GO) analysis of genes with conserved animal or vegetal enrichment, as well as species-specific enrichment in either hemisphere, was also performed (Supplemental Figures S4 and S5). Genes with conserved vegetal localization were enriched in categories associated with germ cell development, regulation of gene expression, and vesicular and lipid transport processes (Supplemental Figure S4). An enrichment of genes in categories associated with reproductive processes was also observed for transcripts with *X. laevis*–specific vegetal localization behavior. In addition, we also noticed enrichment in categories associated with cellular signaling, catabolic processes, and others. Gene ontology analysis for transcripts with *X. tropicalis*–specific vegetal enrichment revealed an enrichment of categories associated with cytoskeleton organization, cell cycle processes, skeletal system development, and protein catabolism. For transcripts with conserved animal enrichment, only one category of biological processes stood out, namely "response to drug," which contains genes encoding for cortactin binding protein 2, a sorting nexin family member, acetyl-CoA carboxylase, and ABC superfamily members (Supplemental Figure S5). *X. laevis*–specific, animally enriched transcripts were enriched in categories associated with protein localization and Ras GTPase signal transduction, as well as nuclear export of mRNAs, whereas animally enriched transcripts from *X. tropicalis* were be enriched in categories associated with transcription of rRNA, mitotic cell cycle, and programmed cell death. Thus we observe a low conservation of GO term categories associated with species-specific animally and vegetally enriched transcripts, respectively.

A

JgiID	gene symbol	RNA seq	qPCR	Localization
Xetrov72004565	*mprip*	-3,05	ND	yes
Xetrov72013870	*xkrx*	-2,95	ND	yes
Xetrov72019787	*ptpn9*	-2,59	-2,72	yes
Xetrov72019410	*smtn*	-2,43	ND	yes
Xetrov72008519	*ano1*	-2,41	ND	yes
Xetrov72009742	*frmd8*	-2,31	ND	yes
Xetrov72029437	*lima1*	-2,31	-3,00	yes
Xetrov72039427	*aen*	-2,21	-2,67	yes
Xetrov72038890	*slc18a1*	-2,07	ND	yes
Xetrov72013759	*fam82a2*	-2,82	-2,90	weak expression
Xetrov72020561	*adpgk*	-2,54	ND	weak expression
Xetrov72030631	*chst10*	-2,48	ND	weak expression
Xetrov72028979	*mcf2l*	-2,26	ND	weak expression
Xetrov72035065	*epdr1*	-2,11	ND	weak expression

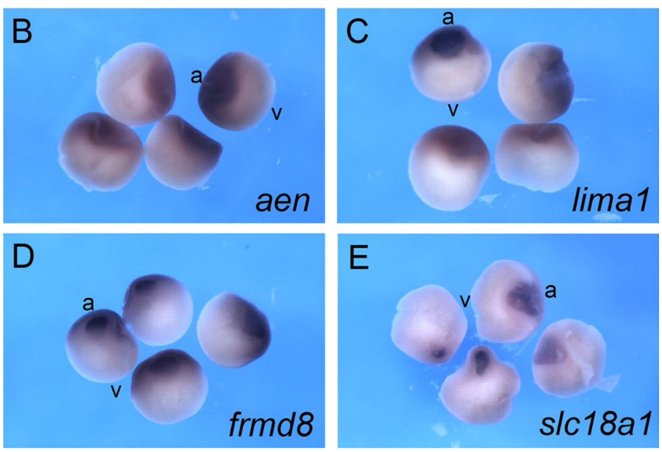

FIGURE 2: Identification of animally enriched RNAs in *X. laevis* oocytes. (A) Fourteen candidate transcripts with at least fourfold animal enrichment were selected for in situ hybridization analysis with *X. laevis* oocytes. JgiID, gene symbol, and relative enrichment in the animal hemisphere (expressed as $\log_2$FC) as revealed by deep sequencing and qPCR analysis. Detection of animal localization by in situ hybridization is indicated. For some of the transcripts, the localization pattern could not be determined due to very low expression levels. (B–E) Animal enrichment as revealed by in situ hybridization for *aen*, *lima*, *frmd8*, and *scl18a1* transcripts. Bisected *X. laevis* stage VI oocytes. Animal (a) and vegetal (v) poles.

Localization activity of endogenous RNAs can be recapitulated for synthetic RNAs injected into *X. laevis* and *X. tropicalis* oocytes

Differential localization behavior of transcripts in the two species analyzed here could be explained by either gain/loss of *cis*-acting RNA localization signals or differences in the *trans*-acting RNA localization machinery. These two possibilities were addressed by microinjection of synthetic RNA fragments from either *X. laevis* or *X. tropicalis* into oocytes from either the same or the other species. The conserved vegetal enrichment of *gdf1* and *grip2* could imply that both the functionality of *cis*-acting RNA signals and *trans*-acting localization proteins have been conserved between species. To test this hypothesis, we injected *X. tropicalis* RNA fragments corresponding to the localization elements (LEs) as identified in *X. laevis* (Mowry and Melton, 1992; Claussen *et al.*, 2011) into early to mid-stage oocytes from *X. laevis* and *X. tropicalis* females and analyzed them for localization by confocal imaging. RNA localization elements from one species also localized in oocytes from the other species, whereas a control RNA (β-*globin* 3′-untranslated region [UTR]) did not localize in oocytes from both species (Figure 5A and Supplemental Figure S6C). RNA localization was quantified as described previously (Bauermeister *et al.*, 2015) and given as average ratio of mean pixel intensity at the vegetal cortex versus mean pixel intensity in the animal cytoplasm (Supplemental Table S9).

Ppp1r2 belongs to the group of RNAs that were vegetally enriched in oocytes from *X. laevis* but not *X. tropicalis* (as described earlier). Because the localization element in *ppp1r2* has not yet been characterized, the complete 3′-UTR was injected, since the vast majority of RNA localization elements have been mapped to this region. The *X. laevis ppp1r2* 3′-UTR indeed mediated vegetal localization after injection into *X. laevis* oocytes (Figure 5B). Vegetal localization was also achieved upon injection into *X. tropicalis* oocytes, showing that the localization machinery in *X. tropicalis* oocytes is able to recognize and mediate transport of the heterologous *X. laevis* RNA. Consistent with the ubiquitous distribution of *ppp1r2* in *X. tropicalis*, as observed by in situ hybridization, the *X. tropicalis* 3′-UTR does not localize upon injection into *X. tropicalis* oocytes or into *X. laevis* oocytes, indicating that it is devoid of a functional localization element. Early-pathway localization activities, with characteristic enrichment in the mitochondrial cloud, were observed upon injection of *X. laevis ppp1r2*-3′-UTR into stage I oocytes, whereas *X. tropicalis ppp1r2*-3′-UTR remains evenly distributed in the cytoplasm or is even excluded from the mitochondrial cloud (Supplemental Figure S6, A and B).

Vegetal localization of *acp6* transcripts has been detected in *X. tropicalis* but not in *X. laevis* oocytes (as described earlier). Injection of *acp6* RNA fragments from *X. laevis* and *X. tropicalis* identified the vegetal localization activity in the 5′-UTR but not in the open reading frame (ORF) or 3′-UTR of the corresponding transcripts (Figure 5C and unpublished data). Of interest, the localization activities found in the injection assay are not consistent with the distribution of the endogenous RNAs in oocytes from the two different species; whereas endogenous *acp6* RNA localizes in *X. tropicalis* oocytes only, injected 5′-UTRs from both species efficiently localized after injection into both *X. laevis* and *X. tropicalis* oocytes (Figure 5C). This finding indicates that the vegetal localization signal of the *X. tropicalis acp6* mRNA could be masked by an unknown mechanism in the context of the full-length transcript.

Assuming that differences in the primary sequence of *cis*-acting vegetal localization elements are responsible for differential localization behavior in the two closely related *Xenopus* species, we compared 3′-UTRs from RNAs with conserved or species-specific localization activity. Indeed, we observe slightly higher degrees of average overall identities with 3′-UTRs from transcripts with conserved vegetal localization than with 3′-UTRs from transcripts with species-specific vegetal enrichment (Supplemental Table S10). However, because sequence identity values scatter widely within the groups of RNAs with conserved and nonconserved localization behavior, this correlation does not appear to provide a predictive value.

The proper localization of orthologous RNAs after injection into oocytes from a different species, as shown for *gdf1*-LE, *grip2*-LE, and *ppp1r2*-3′-UTR, indicates that the *trans*-acting localization machineries acting during vegetal localization seem to be conserved between *X. laevis* and *X. tropicalis*. To test whether similar vegetal localization complexes are assembled in *X. tropicalis* oocytes as described previously for *X. laevis* (Bauermeister *et al.*, 2015), we used a ribonucleoprotein reconstitution approach, using *X. tropicalis* oocyte extracts and in vitro–transcribed early- and late-pathway LEs from *X. laevis* (*gdf1*-LE and *grip2*-LE). With the exception of Stau1 (Allison *et al.*, 2004; Yoon and Mowry, 2004), *X. tropicalis* orthologues of known localization proteins, such as Igf2bp3 (Deshler *et al.*, 1997; Havin *et al.*, 1998), Ptbp1 (Cote *et al.*, 1999), Elavl1 and

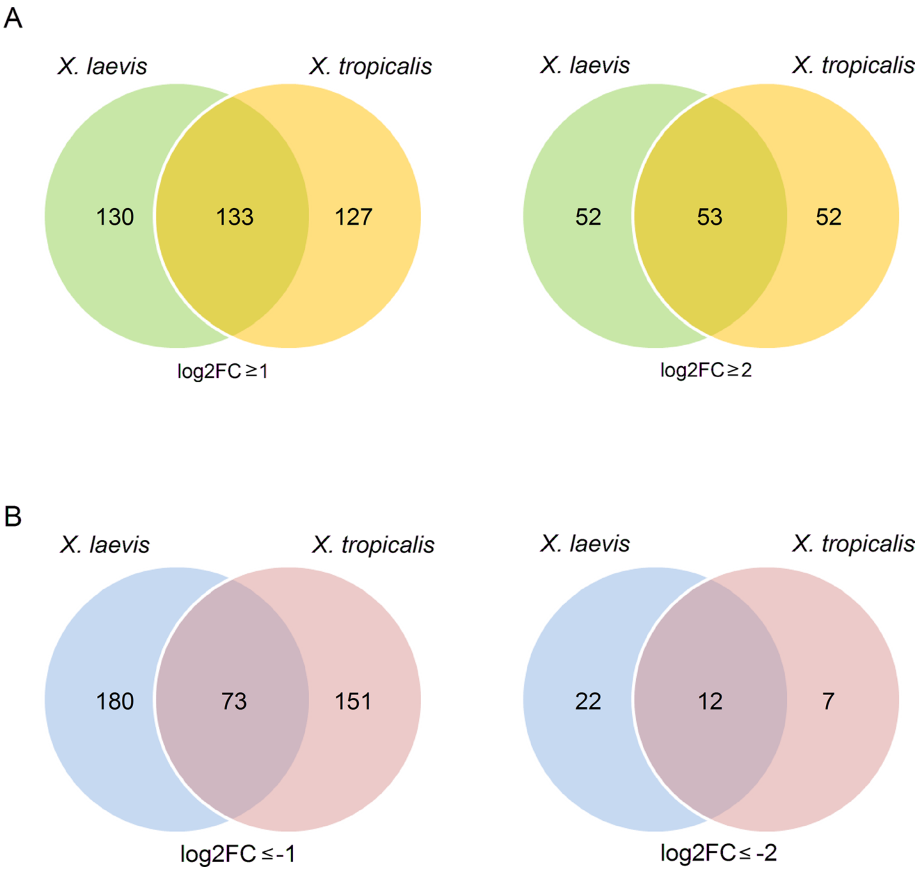

FIGURE 3: Differential RNA distribution is only weakly conserved in a comparison between *X. laevis* and *X. tropicalis.* (A) Numbers of vegetally enriched RNAs from *X. laevis* (green) and *X. tropicalis* (orange) as identified by deep sequencing analysis in the form of Venn diagrams. Thresholds for vegetal localization were set to either $\log_2$FC ≥ 1 (left) or ≥ 2 (right). (B) Numbers of RNAs with animal enrichment in *X. laevis* (blue) and *X. tropicalis* (pink) oocytes in the form of Venn diagrams with thresholds set to $\log_2$FC ≤ 1 (left) and ≤ 2 (right). This comparative analysis was restricted to transcripts with expression in oocytes from both species.

2 (Arthur *et al.*, 2009), and Hnrnpab (Czaplinski *et al.*, 2005), coeluted with *gdf1*- and *grip2*-LE RNAs but not or to a much lesser extent with the β-*globin* control RNA (Figure 6). Comparable protein binding to late-pathways LEs has been observed with *X. laevis* oocyte extracts (Bauermeister *et al.*, 2015). The relatively strong interaction of Stau1 with the control RNA may be explained by a non–sequence-specific interaction of this double-stranded RNA binding domain–containing protein with the stem-loop structures present in the RNA-affinity tag.

In summary, data obtained here suggest that the differential localization behavior of orthologous RNAs is most likely due to differences in the *cis*-acting RNA signal sequences rather than differences in the *trans*-acting RNA localization machineries.

DISCUSSION

In this study, next-generation sequencing techniques were used for the identification of known and novel differentially localized transcripts in oocytes from *X. laevis* and the closely related *X. tropicalis*. Of interest, the overlap of differentially localizing RNAs in a comparison of the two species was found to be much lower than would have been expected from their close evolutionary relationship. Injection analysis suggests that this differential localization behavior is most likely caused by species-specific differences in the *cis*-acting RNA signals rather than in the *trans*-acting localization machineries.

Vegetally localizing RNAs function as important regulators during early *Xenopus* development, and numerous screens have been performed to isolate such transcripts from *Xenopus* oocyte RNA preparations (Rebagliati *et al.*, 1985; Mosquera *et al.*, 1993; Chan *et al.*, 1999; Claussen and Pieler, 2004; Kataoka *et al.*, 2005; Horvay *et al.*, 2006; Cuykendall and Houston, 2010). Here we successfully used next-generation sequencing analysis for the identification of differentially enriched transcripts in *Xenopus* oocytes. Depending on the selected threshold for vegetal enrichment, 140 (at least fourfold enriched) to 350 (at least twofold enriched) different transcripts were identified from *X. laevis* oocytes. This is in good agreement with microarray analysis data, which led to an estimated minimal number of ~275 vegetally localized RNAs (Cuykendall and Houston, 2010). About half of the top 120 enriched sequences identified in the same study were also vegetally enriched in the study described here. However, other RNAs were not enriched by a factor of more than twofold (e.g., *nrf1*, *igf1r*, and *nucks1*) or were found to be even animally enriched (e.g., *exd2*, *sesn1*, and *trim69.1*); thus additional analyses are required to prove vegetal enrichment of candidate genes identified in these various screens, including ours.

About 15–20% of the vegetally enriched transcripts with expression in both *Xenopus* species are encoded by unknown or nonannotated genes; when subjected to gene ontology analysis, the remaining genes were found to group into biological processes such as germ cell development, regulation of gene expression, and vesicular and lipid transport processes. Cellular signaling, catabolic, and other processes were found for transcripts with *X. laevis* unique vegetal enrichment, and cytoskeleton organization, cell cycle processes, skeletal system development, and protein catabolism were identified for transcripts with *X. tropicalis*–specific vegetal enrichment. However, a function of novel localizing transcripts in the given processes remains to be determined.

Although we were able to reidentify almost all of the previously published vegetally localizing RNAs in this study, this was not the case for RNAs with described animal enrichment. In general, the number of highly enriched RNAs (at least eightfold) is much lower for the group of RNAs with animal enrichment than for the group of vegetally enriched RNAs, indicating that animal enrichment in general may not result in a similarly steep gradient of animal–vegetal RNA distribution as shown for vegetally localizing RNAs (King *et al.*, 2005; Sindelka *et al.*, 2010). Because, for a subset of previously described animally localizing RNAs, animal enrichment has been identified in eggs or early embryos (Supplemental Table S3), it cannot be ruled out that differential RNA distribution might also be a result of differential RNA stability that might occur at egg maturation and thus not be detectable in the immature oocytes used in this study. However, animal enrichment has been verified by in situ hybridization as well as qPCR analysis for a group of selected novel candidate

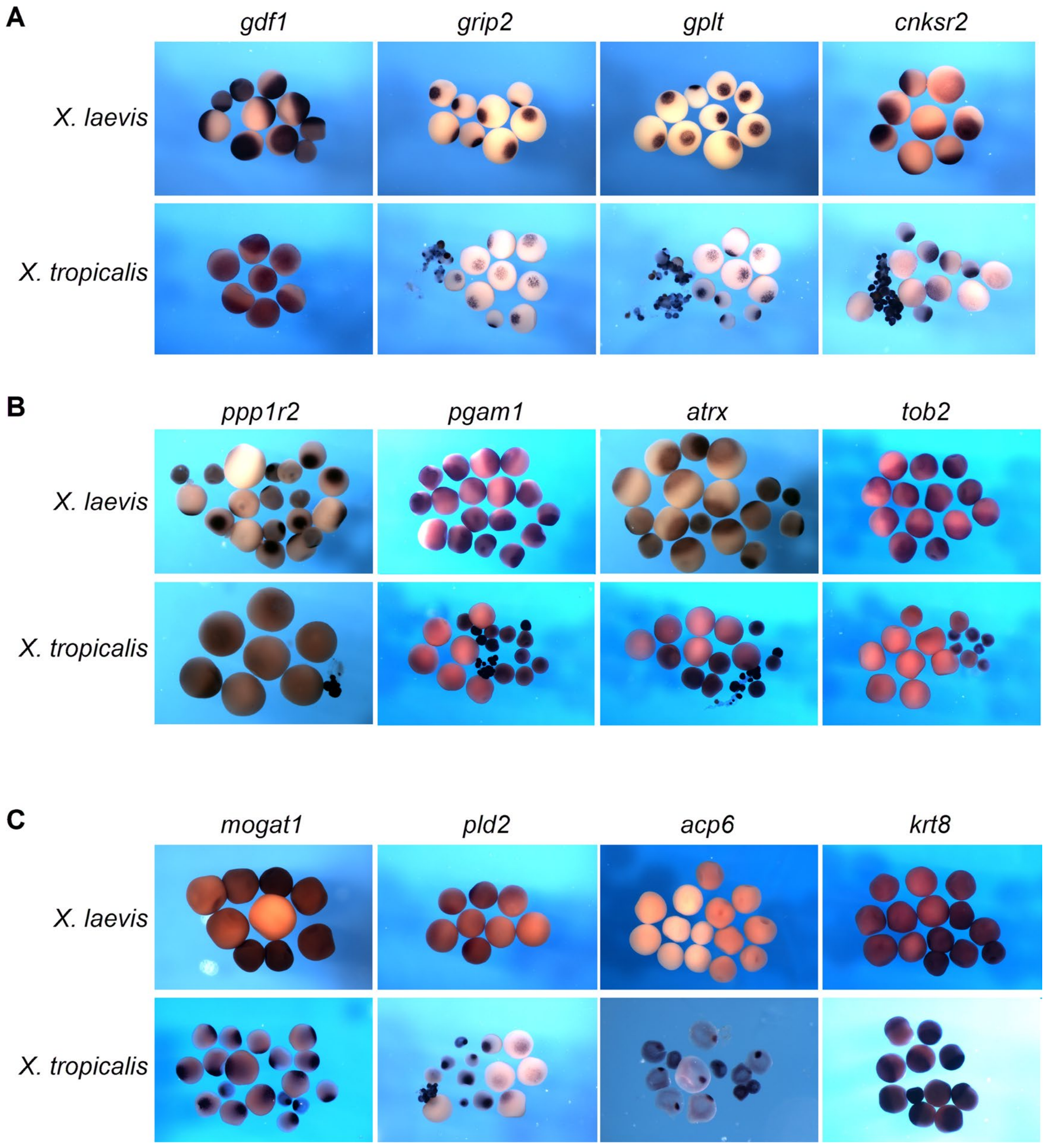

FIGURE 4: Comparative in situ hybridization analysis confirms species-specific localization in *X. laevis* and *X. tropicalis* oocytes. (A–C) In situ hybridization with species-specific antisense RNA probes was performed with stage I–IV oocytes from *X. laevis* and *X. tropicalis.* (A) *Gdf1*, *grip2*, *gplt*, and *cnksr2* localize to the vegetal cortex in both *X. laevis* and *X. tropicalis* oocytes. (B) *Ppp1r2*, *pgam1*, *atrx*, and *tob2* vegetally localize in *X. laevis* only. (C) *Mogat1*, *pld2*, *acp6*, and *krt8* transcripts localize to the vegetal cortex in *X. tropicalis* but not *X. laevis* oocytes.

RNAs in the context of the present study. Knowledge about the effect of animally enriched RNAs on early *Xenopus* development is limited. The animally enriched ubiquitin ligase *trim33* was shown to be essential for ectoderm specification by antagonizing mesoderm-inducing activities, thus allowing for the "default" neural induction (Dupont *et al.*, 2005). Detailed in situ hybridization analysis with newly identified RNAs that exhibit enrichment in animal blastomeres of eight-cell-stage embryos revealed preferential expression of these RNAs in neural ectoderm during later developmental stages, which may indicate a similar function of these RNAs in the establishment of neural fate in ectodermal derivatives (Grant *et al.*, 2014). Gene ontology analysis with animally enriched RNAs identified in this study revealed an enrichment of genes involved in biological processes, such as response to drug for transcripts with conserved animal enrichment, as well as protein and RNA transport, cell cycle processes, and regulation of small GTPase–mediated signal transduction for *X. laevis*–specific, animally enriched RNAs and transcription of rRNA, mitotic cell cycle, and programmed cell death for transcripts with *X. tropicalis*–specific animal enrichment. However, the effect of animally enriched transcripts associated with the aforementioned biological processes on neural ectodermal development in *Xenopus* remains to be determined.

Of interest, our analysis revealed a surprisingly low overlap of differentially enriched RNAs between *X. laevis* and *X. tropicalis* oocytes. These differences in localization behavior could be due to either loss or gain of localization activity in one of the species during

JgiID	Gene symbol	*Xenopus laevis* Deep sequencing Ø (cpm)	*Xenopus laevis* Deep sequencing log_2FC	*Xenopus laevis* qPCR log_2FC	*Xenopus laevis* ISH Localization	*Xenopus tropicalis* Deep sequencing Ø (cpm)	*Xenopus tropicalis* Deep sequencing log_2FC	*Xenopus tropicalis* qPCR log_2FC	*Xenopus tropicalis* ISH Localization
I. RNAs vegetally localizing in *X. laevis* and *X. tropicalis*									
Xetrov72008424	*grip2*	1369	8.34	ND	Early	764	7.18	ND	Early
Xetrov72021968	*gplt*	428	7.88	ND	Early	315	6.49	ND	Early
Xetrov72029018	*cnksr2*	226	2.33	ND	Early	47	1.19	ND	Early
Xetrov72021321	*gdf1*	1379	5.32	3.56	Late	275	3.78	ND	Late
II. RNAs vegetally localizing in *X. laevis* only									
Xetrov72001906	*ppp1r2*	179	2.51	ND	Early	155	0.07	ND	No
Xetrov72026885	*pgam1*	1118	3.98	3.60	Late	320	0.53	–0.07	No
Xetrov72010520	*tob2*	226	2.93	2.31	Late	53	0.52	0.35	No
Xetrov72024723	*atrx*	97	2.37	2.74	Late	247	–0.08	–0.84	No
III. RNAs vegetally localizing in *X. tropicalis* only									
Xetrov72005630	*mogat1*	206	0.29	0.32	No	254	4.87	4.84	Early
Xetrov72003126	*pld2*	163	0.58	ND	No	42	4.79	ND	Early
Xetrov72005805	*acp6*	38	–0.20	0.56	No	21	2.93	2.61	Early
Xetrov72029943	*krt8*	1305	0.28	ND	No	630	1.75	ND	Late

Vegetally enriched RNAs can be grouped into RNAs identified to localize in oocytes from both *X. laevis* and *X. tropicalis* (I), in *X. laevis* only (II), and in oocytes from *X. tropicalis* but not *X. laevis* (III). Candidate vegetally localizing transcripts that were selected for in situ hybridization (ISH) with *X. laevis* and *X. tropicalis* oocytes are listed with JgiID and gene symbol. Average Ø (cpm) per oocyte and relative enrichment in the vegetal hemisphere (expressed as log_2FC) are as shown by deep sequencing analysis and qPCR, respectively. Values below the threshold for vegetal localization of $log_2FC \geq 1$ are indicated in red. Detection of vegetal localization by in situ hybridization and presumptive localization pathway is indicated.

TABLE 1: **Summary of next-generation sequencing, qPCR, and in situ hybridization results for selected known and novel candidate RNAs.**

evolution. However, to address this question, additional information about differential RNA distribution in oocytes from further related frog species is required. Comparative transcriptome analysis revealed strong conservation of temporal gene expression profiles during early development of *X. laevis* and *X. tropicalis*, with the largest differences in expression levels occurring in maternally supplied transcripts. This was consistent with the hourglass model of embryonic patterning (Yanai *et al.*, 2011). According to this model, developmental constraints are highest during mid-embryogenesis, allowing for larger variations in gene expression before and after this critical phase (Kalinka and Tomancak, 2012). The weak conservation of spatial transcript enrichment found in this study might similarly reflect one aspect of higher divergence during early development of the two closely related *Xenopus* species.

Conserved localization behavior is likely to indicate a conserved developmental function of the respective genes in the two *Xenopus* species. However, the absence of conserved spatial RNA enrichment between the relatively closely related species may be due to a certain extent of functional redundancy of localized transcripts, which would have lowered the evolutionary pressure to maintain asymmetric localization of a particular transcript. Alternatively, additional fail-safe mechanisms may ensure restriction of transcripts to specific regions in the developing embryo even if vegetal localization during oogenesis is lost. For example, restriction of *dnd1* and *ddx25* transcripts to primordial germ cells be achieved not only by initial localization to the germplasm during oogenesis, but also by microRNA-mediated clearance of these transcripts in somatic cells and stabilization in the primordial germ cells in the developing embryo (Koebernick *et al.*, 2010; Yamaguchi *et al.*, 2014).

RNA localization assays with heterologous *ppp1r2* 3′-UTRs indicate that differences in the localization behavior are most likely due to alterations in the RNA signal sequence rather than differences in the RNA localization machinery in a comparison of the two *Xenopus* species. Sequence comparisons reveal an overall identity for the *X. laevis* and *X. tropicalis ppp1r2* 3′-UTRs of ~70%, which is above the average sequence identity of ~50% for 3′-UTRs from selected transcripts with differential behavior in the two species. However, even lower sequence identities were revealed for 3′-UTRs or isolated localization elements from RNAs with similar localization behavior in *X. laevis* and *X. tropicalis* (e.g., *gdf1*, *nanos1*). This indicates that differential localization behavior is not necessarily reflected by a lower degree of primary sequence conservation and vice versa. Similarly, it has been shown that even relatively small changes in primary sequence can alter the functional properties of RNA localization elements, either by changing protein binding activities or secondary structure of critical RNA regions (Claussen and Pieler, 2004).

The proper localization of orthologous RNAs after injection into oocytes from a different frog species indicates that the *trans*-acting vegetal localization machineries are conserved. In this context, a detailed comparative analysis of the *gdf1*-LEs from *X. laevis* and the closely related Kenyan clawed frog, *Xenopus borealis*, revealed that *X. borealis* and *X. laevis gdf1*-LE are recognized by the same localization proteins from *X. laevis* oocyte extracts, and both direct vegetal localization after injection into *X. laevis* oocytes (Lewis *et al.*, 2004). Here we demonstrated that a similar set of orthologous localization proteins from *X. tropicalis* oocyte extracts, including Igf2bp3, Ptbp1, Elavl1 and 2, and Hnrnpab, assemble with *X. laevis gdf1*- and *grip2*-LEs, strongly indicating that vegetal localization machineries are conserved between different *Xenopus* species.

Of interest, microinjected *acp6* 5′-UTR did not recapitulate the localization behavior of the endogenous transcript; even though

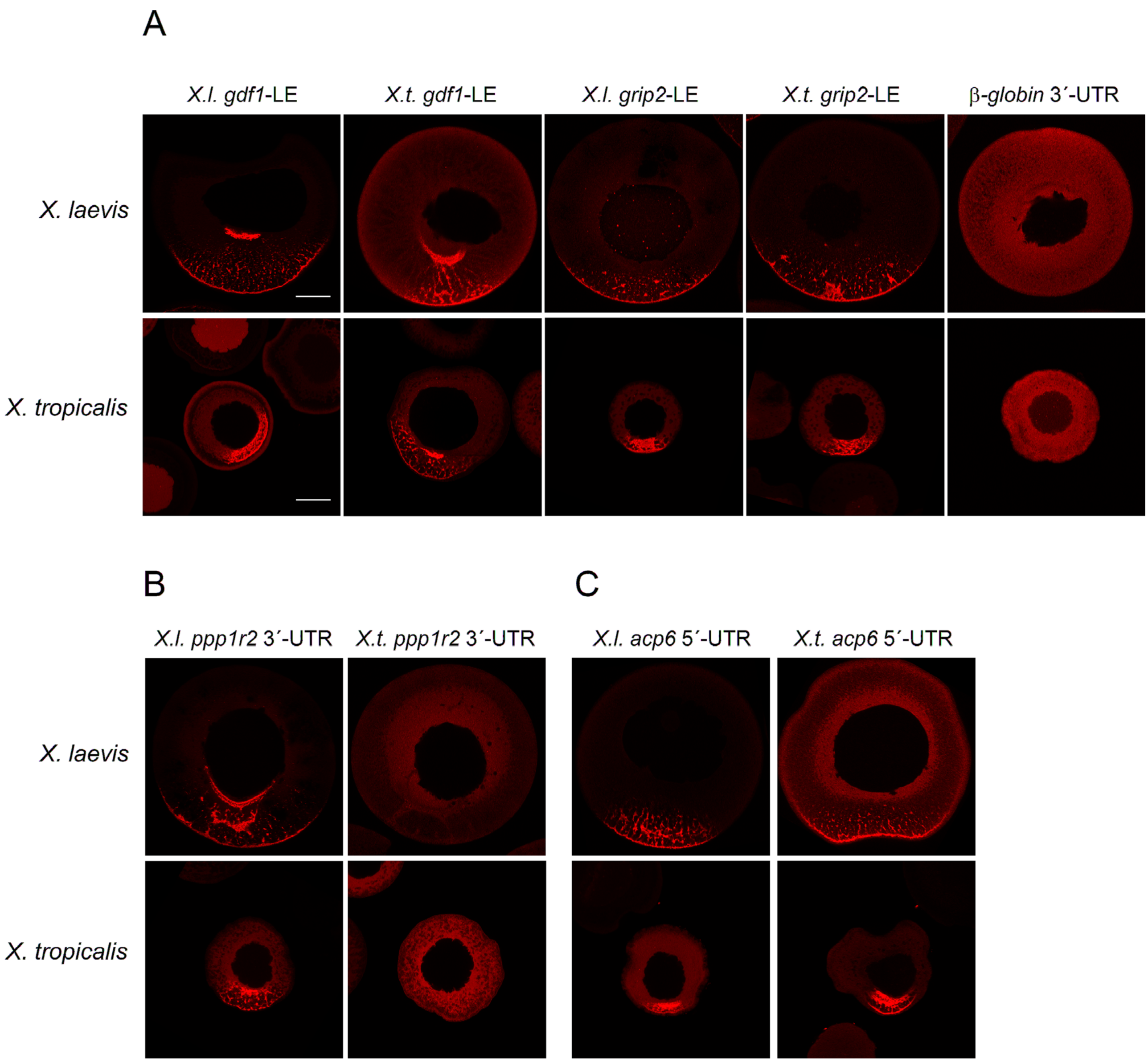

FIGURE 5: Differential localization behavior of orthologous RNAs appears to rely on the RNA signal sequence but not on differences in the RNA localization machinery. (A–C) Isolated localization elements, as well as 5′-UTR, ORF, and 3′-UTRs from different transcripts and species as indicated, were labeled with cyanine-3 and injected into *X. laevis* and *X. tropicalis* oocytes. Representative confocal images of fixed oocytes. Average vegetal/animal ratios of injected RNA are listed in Supplemental Table S9. Vegetal poles are oriented toward the bottom (if assignable). Scale bars, 100 µm. (A) Injection of *gdf1* and *grip2* localization elements from *X. laevis* and *X. tropicalis*, as well as nonlocalizing *β-globin* 3′-UTR (negative control), into oocytes from both species. (B) Injection of *X. laevis and X. tropicalis ppp1r2* 3′-UTRs. (C) Injection of *X. laevis and X. tropicalis acp6*-5′-UTRs.

acp6 does not localize to the vegetal cortex in *X. laevis* oocytes, injected 5′-UTR mediates vegetal localization in oocytes from both species. This could indicate that the localization element of the *X. tropicalis acp6* transcript is masked in the context of the full-length transcript. However, it has not been possible to identify this "masking activity" in the adjacent coding region (unpublished data), and it will be interesting to examine why such an inhibiting activity would be present in the 3′-UTR. Alternatively, vegetal localization of endogenous *X. laevis acp6* transcripts may be inhibited by competition with other localizing RNAs for limiting components of the *trans*-acting localization machinery, as injection of high amounts of synthetic RNA may have uncovered this cryptic localization activity.

MATERIALS AND METHODS

RNA preparation from *X. laevis* and *X. tropicalis* oocytes

X. laevis and *X. tropicalis* ovaries were obtained by surgery from adult females and subjected to collagenase treatment (Liberase; Roche Diagnostics, Mannheim, Germany). Animal and vegetal oocyte halves were prepared by manual dissection using a scalpel blade and snap frozen in liquid nitrogen. RNA was prepared from either 10 or 30 animal and vegetal halves as described (Claussen and Pieler, 2004). Briefly, animal and vegetal halves were homogenized in RNA extraction buffer (50 mM Tris/HCl, pH 7.5, 5 mM EDTA, pH 8.0, 40 mM NaCl, 0.5% SDS) containing proteinase K (Merck, Darmstadt, Germany) and incubated for 1 h at 45°C, followed

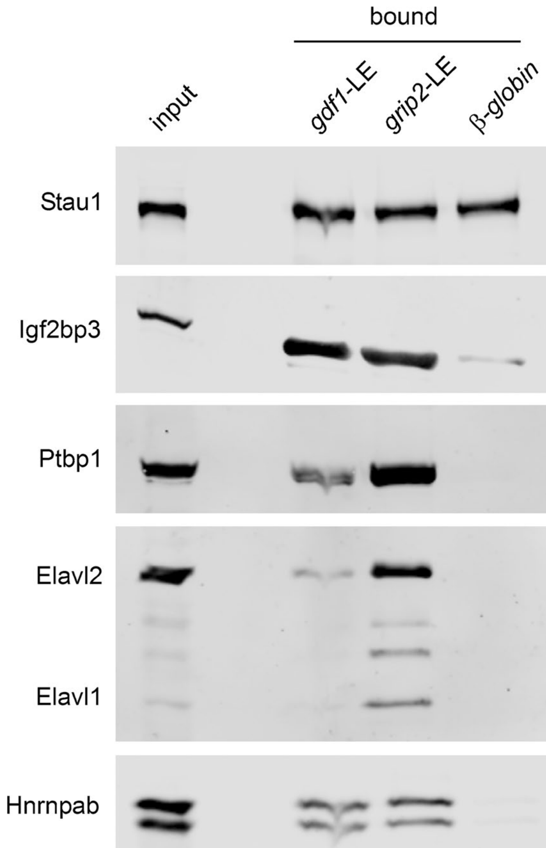

FIGURE 6: Interaction of localization proteins with LE-RNAs is conserved in *X. tropicalis*. Assembly of localization complexes with *X. tropicalis* oocyte extracts and tagged *X. laevis gdf1*-LE, *grip2*-LE, and *β-globin*-3′-UTR control RNA was performed in vitro. Copurifying localization proteins were detected by Western blot analysis.

by several extraction steps with acidic phenol/chloroform/isoamyl alcohol and chloroform/isoamyl alcohol. Afterward, the RNA was precipitated by addition of an equal volume of 8 M LiCl. After being dissolve and reprecipitated with ammonium acetate/ethanol, the RNA was treated with DNase (Thermo Scientific, Waltham, MA).

RNA sequencing, data processing, and statistical analysis

For sequencing, the RNA samples were prepared with the TruSeq RNA Sample Prep Kit, version 2, according to the manufacturer's instructions (Illumina, San Diego,CA) and sequenced using a HiSeq 2000 (Illumina). For *X. laevis* samples, 95–base pair paired-end runs were performed, whereas *X. tropicalis* samples were analyzed by 50–base pair single-end runs. Sequencing quality was checked via FastQC software (www.bioinformatics.babraham.ac.uk/projects/fastqc/). Sequence images were transformed to BCL files with the Illumina BaseCaller software and demultiplexed to FASTQ files with CASAVA, version 1.8.2. Duplicated reads were not removed. To allow for direct comparison, sequences from both experimental setups (*X. laevis* and *X. tropicalis*) were aligned to the transcript reference sequence of *X. tropicalis* (by courtesy of Michael J. Gilchrist: http://genomics.nimr.mrc.ac.uk/resources/xenopus/Xt-transcripts-Xenbase-v72b-MJG-27oct11.fasta), taking unique gene identifiers only. Read mapping was performed with Bowtie2, version 2.1.0, using the "very sensitive" local alignment mode and standard parameters for alignment scoring (Langmead and Salzberg, 2012). Roughly, this allows up to six mismatches (12%) in reads of 50 base pairs and 39 mismatches (~21%) in 2× 95–base pair paired-end reads. Subsequently conversion of resulting .sam files to sorted .bam files, indexing, and filtering of unique hits (MAPQ value >20, "-q20") was conducted with Samtools, version 0.1.19. Counting of hits to transcript was performed using the Samtools idxstat function (with subsequent halving of counts for paired-end reads). Data were preprocessed and analyzed in the R/Bioconductor environment (www.bioconductor.org), loading edgeR and biomaRt packages (Robinson *et al.*, 2010). After filtering, genes with >50 counts for at least half of the samples were selected and normalized to trimmed mean of *M* values and dispersions estimated. Furthermore, genes were filtered for group (animal and vegetal) means >50 counts and tested for differentially expressed genes based on a generalized linear model likelihood ratio test, assuming negative binomial data distribution via edgeR. For comparability between the two different data sets (*X. laevis* and *X. tropicalis*), counts per million (cpm) were calculated, and thresholds were set to mean cpm for at least one group (animal or vegetal) in each data set ≥5. Fold changes (ratios) between animal and vegetal hemispheres were calculated as $\log_2$ values ($\log_2$FC). Gene annotation was enriched by data from Xenbase. The assignment to previously identified vegetally enriched candidate genes was performed by BLAST searches (Altschul *et al.*, 1990) of the *X. tropicalis* reference sequence collection with UniGeneID sequences from Cuykendall and Houston (2010), as well as candidate sequences from our own microarray screen (unpublished results). The data discussed in this article have been deposited in the National Center for Biotechnology Information Gene Expression Omnibus and are accessible through GEO Series accession number GSE58420 (Edgar *et al.*, 2002).

Gene ontology term analysis

GO term analysis was performed using the functional annotation tool of DAVID, version 6.7 (Huang da *et al.*, 2009a,b). *Homo sapiens*, *Mus musculus*, *X. laevis*, *X. tropicalis*, *D. rerio*, and *Drosophila melanogaster* were selected to limit annotations of the gene list, and *H. sapiens* was selected as population background. GO term analysis was performed on gene lists of transcripts with conserved and species-specific animal or vegetal enrichment.

Pairwise sequence alignments

Pairwise global nucleotide sequence alignments were performed with EMBOSS Needle, applying the default alignment settings (Rice *et al.*, 2000).

Cloning procedures

For verification of differential RNA localization, in situ hybridization with *X. laevis* and *X. tropicalis* oocytes was performed. Gene- and species-specific in situ hybridization probes were generated by cloning of the corresponding cDNA fragments into pGEM-Teasy (Promega, Madison, WI). Primers were designed to match the corresponding nucleotide reference sequence listed in Xenbase (Supplemental Table S11). In cases in which no gene had been assigned to the corresponding JgiID sequence, BLAST searches (Altschul *et al.*, 1990) with these sequences were performed and primers designed for the best-matching expressed sequence tag (EST) sequence from *X. laevis*/*X. tropicalis*. GenBank accession numbers of these transcripts are given in the respective tables and figures. The sequence with the JgiID Xetrov72021968 best matched to ESTs DY566077 (*X. laevis*) and BX772720 (*X. tropicalis*) and was named *germ plasm localized transcript* (*gplt*) according to the localization observed in oocytes from both *Xenopus* species.

For the generation of Cy3-labeled and *lacZ*-tagged injection constructs, cDNA fragments corresponding to the 5′-UTR, ORF, 3′-UTR, or localization sequence were amplified by PCR and cloned into *Bam*HI/*Xho*I or *Eco*RI sites of pBK-CMV-lacZ (Claussen and Pieler, 2004). Oligonucleotides used for cloning of cDNA subfragments into pBK-CMV-lacZ are listed in Supplemental Table S12.

Quantitative RT-PCR analysis

To assess the relative enrichment of candidate RNAs in either animal or vegetal hemispheres, quantitative RT analysis using the iQ SYBR Green Super Mix and CFX 96 Real-Time PCR Detection System (Bio-Rad, Hercules, CA) was performed on the RNA preparations as for RNA sequencing analysis. Mean relative enrichments were determined for two biological replicates and two technical replicates, respectively, and are given as $\log_2$FC. Oligonucleotides used for quantitative RT-PCR analysis are listed in Supplemental Table S13.

In situ hybridization analysis

In situ hybridization analysis on *X. laevis* and *X. tropicalis* oocytes was as described (Harland, 1991; Hollemann *et al.*, 1999) using digoxigenin-labeled antisense RNA probes.

In vitro synthesis of cyanine-3– and Atto-633–labeled transcripts and RNA localization assays

In vitro synthesis of cyanine-3–labeled transcripts and oocyte injection was as described (Claussen and Pieler, 2010). For synthesis of Atto-633–labeled transcripts, 1 nmol of aminoallyl-UTP-Atto-633 (NU-821-633; Jena Bioscience, Jena, Germany) was added to a 25 µl of in vitro transcription reaction. In contrast to the previously used protocols, *X. laevis* and *X. tropicalis* mid-stage oocytes were incubated in vitellogenin-free oocyte culture medium after injection and analyzed by confocal microscopy using the LSM 780 (Zeiss, Oberkochen, Germany). Fixation, clearing, and imaging of injected oocytes were done as described in Gagnon and Mowry (2011). Quantification of vegetal enrichment was performed as described previously (Bauermeister *et al.*, 2015). In brief, confocal images of injected oocytes were opened in ImageJ (National Institutes of Health, Bethesda, MD), and mean pixel intensities at the vegetal cortex and in the animal cytoplasm were measured by using the segmented line tool and used to calculate the average vegetal/animal ratio of pixel intensity. For transcripts with no vegetal localization activity, the assignment of animal and vegetal poles is hampered. In these cases, mean pixel intensities of arbitrarily defined opposite cytoplasmic regions were used for quantification.

RNA affinity purification

For in vitro assembly of localization complexes from *X. tropicalis* oocyte extracts, *X. laevis gdf1*- and *grip2*-LEs were cloned into *Bam*HI/*Xho*I sites of the PP7 RNA-tag–containing pBluescript II derivative (Bauermeister *et al.*, 2015). *Xho*I-linearized plasmids were used as templates for T7-mediated in vitro synthesis of PP7-tagged RNAs (MEGA script T7; Ambion; Thermo Scientific). Gdf1-LE, grip2-LE, and β-globin 3′-UTRs were immobilized on ZZ-tev-PP7coat protein bound immunoglobulin G–agarose, and RNA affinity purification was essentially as described previously (Bauermeister *et al.*, 2015). For the preparation of *X. tropicalis* oocyte S16 extracts, ~250 µl of early- and late-stage oocytes were homogenized in 500 µl of IPP145 buffer (50 mM Tris-HCl, pH 8, 145 mM NaCl, 5% glycerol, 0.05% NP-40 substitute, 1 mM dithiothreitol) with protease inhibitors (Complete; Roche) and centrifuged for 30 min at 16,000 × *g*. Reconstitution of localization complexes and washing and elution steps were all performed in IPP145 buffer. S16 input and eluates were subsequently analyzed by Western blot for copurification of *X. tropicalis* localization proteins using the following antibodies: anti-Igf2bp3 (Zhang *et al.*, 1999), 1:5000; anti-Ptbp1 (4E11; BSBS Antibody Facility, Braunschweig, Germany), 1:10; anti-HuR (sc-5261; Santa Cruz Biotechnology, Dallas, TX), 1:5000; anti-Hnrnpab (Czaplinski *et al.*, 2005), 1:10,000; and anti-Stau1 (Allison *et al.*, 2004), 1:5000. All antibodies showed cross-reactivity with orthologous proteins from *X. tropicalis*. Secondary IRDye 680– or 800–labeled anti-mouse and anti-rabbit antibodies (Li-Cor, Lincoln, NE) were used at 1:20,000 dilutions and detection was performed using a Li-Cor Odyssey infrared imaging system.

Note added in proof. While the manuscript was under review, De Domenico *et al.* (2015) reported on the spatial distribution of maternal mRNAs in the *X. tropicalis* eight-cell-stage embryo as revealed by single-blastomere sequencing. The vast majority of novel transcripts with consistent differential enrichment reported in their analysis were also identified to be asymmetrically distributed in our study.

ACKNOWLEDGMENTS

We thank Mike Gilchrist for providing access to the *X. tropicalis* transcript reference sequence collection and helpful advice during the initial phase of this study, as well as Gregor Bucher for discussions and Marion Dornwell for excellent technical assistance. Antibodies were kindly provided by J. Yisraeli (Igf2bp3), K. Czaplinski and I.W. Mattaj (Hnrnpab), and N. Standart (Stau1).

REFERENCES

Allison R, Czaplinski K, Git A, Adegbenro E, Stennard F, Houliston E, Standart N (2004). Two distinct Staufen isoforms in Xenopus are vegetally localized during oogenesis. RNA 10, 1751–1763.

Altschul SF, Gish W, Miller W, Myers EW, Lipman DJ (1990). Basic local alignment search tool. J Mol Biol 215, 403–410.

Arthur PK, Claussen M, Koch S, Tarbashevich K, Jahn O, Pieler T (2009). Participation of Xenopus Elr-type proteins in vegetal mRNA localization during oogenesis. J Biol Chem 284, 19982–19992.

Bally-Cuif L, Schatz WJ, Ho RK (1998). Characterization of the zebrafish Orb/CPEB-related RNA binding protein and localization of maternal components in the zebrafish oocyte. Mech Dev 77, 31–47.

Bauermeister D, Claussen M, Pieler T (2015). A novel role for Celf1 in vegetal RNA localization during Xenopus oogenesis. Dev Biol 405, 214–224.

Beckham YM, Nath K, Elinson RP (2003). Localization of RNAs in oocytes of Eleutherodactylus coqui, a direct developing frog, differs from Xenopus laevis. Evol Dev 5, 562–571.

Betley JN, Heinrich B, Vernos I, Sardet C, Prodon F, Deshler JO (2004). Kinesin II mediates Vg1 mRNA transport in Xenopus oocytes. Curr Biol 14, 219–224.

Bewick AJ, Chain FJ, Heled J, Evans BJ (2012). The pipid root. Syst Biol 61, 913–926.

Bossuyt F, Roelants K (2009). Frogs and toads (Anura). In: The Timetree of Life, ed. SB Hedges and S Kumar, Oxford, UK: Oxford University Press, 357–364.

Chan AP, Kloc M, Etkin LD (1999). fatvg encodes a new localized RNA that uses a 25-nucleotide element (FVLE1) to localize to the vegetal cortex of Xenopus oocytes. Development 126, 4943–4953.

Chang P, Torres J, Lewis RA, Mowry KL, Houliston E, King ML (2004). Localization of RNAs to the mitochondrial cloud in Xenopus oocytes through entrapment and association with endoplasmic reticulum. Mol Biol Cell 15, 4669–4681.

Claussen M, Pieler T (2004). Xvelo1 uses a novel 75-nucleotide signal sequence that drives vegetal localization along the late pathway in Xenopus oocytes. Dev Biol 266, 270–284.

Claussen M, Pieler T (2010). Identification of vegetal RNA-localization elements in Xenopus oocytes. Methods 51, 146–151.

Claussen M, Tarbashevich K, Pieler T (2011). Functional dissection of the RNA signal sequence responsible for vegetal localization of XGrip2.1 mRNA in Xenopus oocytes. RNA Biol 8, 873–882.

Cote CA, Gautreau D, Denegre JM, Kress TL, Terry NA, Mowry KL (1999). A Xenopus protein related to hnRNP I has a role in cytoplasmic RNA localization. Mol Cell 4, 431–437.

Cuykendall TN, Houston DW (2010). Identification of germ plasm-associated transcripts by microarray analysis of Xenopus vegetal cortex RNA. Dev Dyn 239, 1838–1848.

Czaplinski K, Kocher T, Schelder M, Segref A, Wilm M, Mattaj IW (2005). Identification of 40LoVe, a Xenopus hnRNP D family protein involved in localizing a TGF-beta-related mRNA during oogenesis. Dev Cell 8, 505–515.

De Domenico E, Owens ND, Grant IM, Gomes-Faria R, Gilchrist MJ (2015). Molecular asymmetry in the 8-cell stage Xenopus tropicalis embryo described by single blastomere transcript sequencing. Dev Biol 2015, pii: S0012-1606(15)30015-4.

Deshler JO, Highett MI, Schnapp BJ (1997). Localization of Xenopus Vg1 mRNA by Vera protein and the endoplasmic reticulum. Science 276, 1128–1131.

Dupont S, Zacchigna L, Cordenonsi M, Soligo S, Adorno M, Rugge M, Piccolo S (2005). Germ-layer specification and control of cell growth by Ectodermin, a Smad4 ubiquitin ligase. Cell 121, 87–99.

Edgar R, Domrachev M, Lash AE (2002). Gene Expression Omnibus: NCBI gene expression and hybridization array data repository. Nucleic Acids Res 30, 207–210.

Elinson RP, Sabo MC, Fisher C, Yamaguchi T, Orii H, Nath K (2011). Germ plasm in Eleutherodactylus coqui, a direct developing frog with large eggs. EvoDevo 2, 20.

Gagnon JA, Kreiling JA, Powrie EA, Wood TR, Mowry KL (2013). Directional transport is mediated by a Dynein-dependent step in an RNA localization pathway. PLoS Biol 11, e1001551.

Gagnon JA, Mowry KL (2011). Visualization of mRNA localization in Xenopus oocytes. Methods Mol Biol 714, 71–82.

Grant PA, Yan B, Johnson MA, Johnson DL, Moody SA (2014). Novel animal pole-enriched maternal mRNAs are preferentially expressed in neural ectoderm. Dev Dyn 243, 478–496.

Gururajan R, Perry-O'Keefe H, Melton DA, Weeks DL (1991). The Xenopus localized messenger RNA An3 may encode an ATP-dependent RNA helicase. Nature 349, 717–719.

Harland RM (1991). In situ hybridization: an improved whole-mount method for Xenopus embryos. Methods Cell Biol 36, 685–695.

Havin L, Git A, Elisha Z, Oberman F, Yaniv K, Schwartz SP, Standart N, Yisraeli JK (1998). RNA-binding protein conserved in both microtubule- and microfilament-based RNA localization. Genes Dev 12, 1593–1598.

Hollemann T, Panitz F, Pieler T (1999). In situ hybridization techniques with Xenopus embryos. In: A Comparative Methods Approach to the Study of Oocytes and Embryos, ed. JD Richter, Oxford, UK: Oxford University Press, 279–290.

Horvay K, Claussen M, Katzer M, Landgrebe J, Pieler T (2006). Xenopus Dead end mRNA is a localized maternal determinant that serves a conserved function in germ cell development. Dev Biol 291, 1–11.

Houston DW (2013). Regulation of cell polarity and RNA localization in vertebrate oocytes. Int Rev Cell Mol Biol 306, 127–185.

Howley C, Ho RK (2000). mRNA localization patterns in zebrafish oocytes. Mech Dev 92, 305–309.

Huang da W, Sherman BT, Lempicki RA (2009a). Bioinformatics enrichment tools: paths toward the comprehensive functional analysis of large gene lists. Nucleic Acids Res 37, 1–13.

Huang da W, Sherman BT, Lempicki RA (2009b). Systematic and integrative analysis of large gene lists using DAVID bioinformatics resources. Nat Protoc 4, 44–57.

Imbrie GA, Wu H, Seldin DC, Dominguez I (2012). Asymmetric localization of Ck2α during Xenopus oogenesis. Hum Genet Embryol Suppl 4, 11328.

Kalinka AT, Tomancak P (2012). The evolution of early animal embryos: conservation or divergence? Trends Ecol Evol 27, 385–393.

Kataoka K, Tazaki A, Kitayama A, Ueno N, Watanabe K, Mochii M (2005). Identification of asymmetrically localized transcripts along the animal-vegetal axis of the Xenopus egg. Dev Growth Differ 47, 511–521.

King ML, Messitt TJ, Mowry KL (2005). Putting RNAs in the right place at the right time: RNA localization in the frog oocyte. Biol Cell 97, 19–33.

Kloc M, Spohr G, Etkin LD (1993). Translocation of repetitive RNA sequences with the germ plasm in Xenopus oocytes. Science 262, 1712–1714.

Koebernick K, Loeber J, Arthur PK, Tarbashevich K, Pieler T (2010). Elr-type proteins protect Xenopus Dead end mRNA from miR-18-mediated clearance in the soma. Proc Natl Acad Sci USA 107, 16148–16153.

Kosaka K, Kawakami K, Sakamoto H, Inoue K (2007). Spatiotemporal localization of germ plasm RNAs during zebrafish oogenesis. Mech Dev 124, 279–289.

Langmead B, Salzberg SL (2012). Fast gapped-read alignment with Bowtie 2. Nat Methods 9, 357–359.

Lewis RA, Kress TL, Cote CA, Gautreau D, Rokop ME, Mowry KL (2004). Conserved and clustered RNA recognition sequences are a critical feature of signals directing RNA localization in Xenopus oocytes. Mech Dev 121, 101–109.

Linnen JM, Bailey CP, Weeks DL (1993). Two related localized mRNAs from Xenopus laevis encode ubiquitin-like fusion proteins. Gene 128, 181–188.

Maegawa S, Yasuda K, Inoue K (1999). Maternal mRNA localization of zebrafish DAZ-like gene. Mech Dev 81, 223–226.

Messitt TJ, Gagnon JA, Kreiling JA, Pratt CA, Yoon YJ, Mowry KL (2008). Multiple kinesin motors coordinate cytoplasmic RNA transport on a subpopulation of microtubules in Xenopus oocytes. Dev Cell 15, 426–436.

Mosquera L, Forristall C, Zhou Y, King ML (1993). A mRNA localized to the vegetal cortex of Xenopus oocytes encodes a protein with a nanos-like zinc finger domain. Development 117, 377–386.

Mowry KL, Melton DA (1992). Vegetal messenger RNA localization directed by a 340-nt RNA sequence element in Xenopus oocytes. Science 255, 991–994.

Nath K, Boorech JL, Beckham YM, Burns MM, Elinson RP (2005). Status of RNAs, localized in Xenopus laevis oocytes, in the frogs Rana pipiens and Eleutherodactylus coqui. J Exp Zool B Mol Dev Evol 304, 28–39.

Rebagliati MR, Weeks DL, Harvey RP, Melton DA (1985). Identification and cloning of localized maternal RNAs from Xenopus eggs. Cell 42, 769–777.

Rice P, Longden I, Bleasby A (2000). EMBOSS: the European Molecular Biology Open Software Suite. Trends Genet 16, 276–277.

Robinson MD, McCarthy DJ, Smyth GK (2010). edgeR: a Bioconductor package for differential expression analysis of digital gene expression data. Bioinformatics 26, 139–140.

Sater KA, Gilchrist MJ (2012). Xenopus genomics and genetics: progress and prospects. In: Genome Mapping and Genomics in Laboratory Animals, ed. P Denny and C Kole, Berlin: Springer-Verlag, 183–196.

Sindelka R, Sidova M, Svec D, Kubista M (2010). Spatial expression profiles in the Xenopus laevis oocytes measured with qPCR tomography. Methods 51, 87–91.

Snedden DD, Bertke MM, Vernon D, Huber PW (2013). RNA localization in Xenopus oocytes uses a core group of trans-acting factors irrespective of destination. RNA 19, 889–895.

Suzuki H, Maegawa S, Nishibu T, Sugiyama T, Yasuda K, Inoue K (2000). Vegetal localization of the maternal mRNA encoding an EDEN-BP/Bruno-like protein in zebrafish. Mech Dev 93, 205–209.

White JA, Heasman J (2008). Maternal control of pattern formation in Xenopus laevis. J Exp Zool B Mol Dev Evol 310, 73–84.

Yamaguchi T, Kataoka K, Watanabe K, Orii H (2014). Restriction of the Xenopus DEADSouth mRNA to the primordial germ cells is ensured by multiple mechanisms. Mech Dev 131, 15–23.

Yanai I, Peshkin L, Jorgensen P, Kirschner MW (2011). Mapping gene expression in two Xenopus species: evolutionary constraints and developmental flexibility. Dev Cell 20, 483–496.

Yoon YJ, Mowry KL (2004). Xenopus Staufen is a component of a ribonucleoprotein complex containing Vg1 RNA and kinesin. Development 131, 3035–3045.

Zhang Q, Yaniv K, Oberman F, Wolke U, Git A, Fromer M, Taylor WL, Meyer D, Standart N, Raz E, Yisraeli JK (1999). Vg1 RBP intracellular distribution and evolutionarily conserved expression at multiple stages during development. Mech Dev 88, 101–106.

Zhou Y, Zhang J, King ML (2004). Polarized distribution of mRNAs encoding a putative LDL receptor adaptor protein, xARH (autosomal recessive hypercholesterolemia) in Xenopus oocytes. Mech Dev 121, 1249–1258.